

## 15.B.2

# EXPLOITING NWRT PAR CAPABILITIES TO IMPROVE TEMPORAL DATA RESOLUTION

Pamela L. Heinselman<sup>\*</sup>  
NOAA/National Severe Storms Laboratory, Norman, Oklahoma

Sebastian Torres  
OU CIMMS and NOAA/NSSL, Norman, Oklahoma

## 1. INTRODUCTION

Since May 2004, scientists at the National Severe Storms Laboratory (NSSL) have been exploring the high-temporal resolution weather scanning capabilities of an S-band (9.38 cm), agile-beam, PAR system. Located in Norman, OK, this system is referred to as the National Weather Radar Testbed Phased Array Radar (NWRT PAR). The system is part of the broader multifunction phased array radar (MPAR) initiative that is investigating the use of a single radar system to perform both weather and aircraft surveillance functions (Weber et al. 2007; National Academies 2008). Interested readers may read Znić et al. (2007) for a detailed, technical description of the NWRT PAR.

A key capability of PAR technology is high-temporal resolution sampling that can be achieved through many methods. As illustrated in Heinselman et al. (2008), data collection with the NWRT PAR over a 90° sector, rather than over a typical 360° sector, produces faster updates than would otherwise be possible. Because a future operational system would likely have a multi-panel design that samples a full 360° sector, the NWRT PAR demonstrates this design-driven rapid-scan capability. Moreover, the NWRT PAR's electronic steering allows the development of unique sampling techniques like beam multiplexing (Yu et al. 2007) and weather-focused electronic adaptive scanning that can further reduce sampling time.

This paper provides an analysis of the tradeoffs involved in the design of rapid scanning strategies, describes the electronic adaptive scanning technique currently implemented on the NWRT PAR, and illustrates examples of sampling tradeoffs employed by this unique radar system. Although most of the tradeoff analysis can be extended to other radar systems, the focus of this work is on the NWRT PAR.

---

*\*Corresponding author address:* Pamela Heinselman, NSSL, 120 David L. Boren Blvd., Norman, OK 73072  
email: Pam.Heinselman@noaa.gov

## 2. NWRT PAR

Briefly, the NWRT PAR exploits a passive, 4352-element S-band phased-array antenna to provide stationary, three-dimensional electronic scanning of weather echoes within a given 90° azimuthal sector. The antenna is mounted on a turntable to allow focused data collection in the direction of greatest meteorological interest. The antenna beamwidth is 1.5° at boresite (i.e., perpendicular to the array plane) and gradually increases to 2.1° at ±45° from boresite. The peak transmitted power is 750 kW and the range resolution provided by this system is 240 m. In some aspects, such as beamwidth and sensitivity, the NWRT PAR is inferior compared to operational radars such as the Weather Surveillance Radar-1988 Doppler (WSR-88D). However, the purpose of this system is not to achieve operational-like performance or to serve as a prototype for the MPAR, but to demonstrate the operational utility of some of the unique capabilities offered by PAR technology that may eventually drive the design of future operational weather radars.

Significant hardware and software upgrades have been and are needed to support the NWRT mission as a demonstrator system for the MPAR concept. As described in Torres et al. (2010), since 2007 scientists and engineers at NSSL have been improving the functionality and capabilities of the NWRT PAR, including data quality and the development of electronic adaptive scanning (section 4).

## 3. DESIGN OF SCANNING STRATEGIES FOR THE NWRT PAR

Pulsed weather radars continuously sample the atmosphere in three dimensions, and scanning strategies are used to control how this sampling occurs. The effective design of scanning strategies involves tailoring spatial sampling and data acquisition parameters for a specific need or particular meteorological situation. Herein we discuss the considerations and tradeoffs involved in the design of scanning strategies. Although most of this analysis can be extended to other radar systems, the focus is on the NWRT PAR.

Spatial sampling occurs on a volumetric grid defined on spherical coordinates: range, azimuth, and elevation. The grid spacing in range is controlled by the sampling period of echoes at the radar receiver, and grid spacing is usually chosen to match the depth of the radar's resolution volume to produce independent estimates of meteorological variables along the beam (Doviak and Zrnić 2006). However, oversampling in range can be used to reduce the uncertainty of weather data without increasing update times (Torres and Zrnić 2003). In the NWRT PAR, typical range spacing is 240 m, though the system can oversample by factors of 4, 8, or 16. The main tradeoff associated with range oversampling is related to the data throughput and computational complexity that are required with finer sampling. On the other hand, sampling in azimuth and elevation determines the number of beam positions in the scanning strategy and lead to more fundamental tradeoffs discussed next.

The scan update time ( $UT$ ) is defined as the time to complete the execution of a scanning strategy and can be computed as

$$UT = \sum_{i=1}^{BP} DT_i, \quad (1)$$

where  $BP$  is the number of beam positions in the scanning strategy and  $DT_i$  is the dwell time corresponding to the  $i$ -th beam position. This equation shows that the scan update time is directly proportional to the number of antenna beam positions in the scanning strategy which, in turn, is dictated by the sampling in azimuth and elevation.

The azimuthal sampling is usually set to match the antenna beamwidth so that complete coverage can be obtained with the minimum number of beam positions. Nevertheless, oversampling (i.e., overlapped beams) can be used advantageously once again; in this case, to improve observations of small-scale features at long ranges such as with super-resolution on the WSR-88D network (Brown et al. 2002, Torres and Curtis 2007). Because the NWRT PAR's antenna is stationary during data collection, finer azimuthal spacing can provide improved estimates of reflectivity and velocity magnitude, and as a result improved depictions of storm structure. The azimuthal beam resolution, however, remains unchanged. The number of beam positions in azimuth is determined by the extent of coverage and the desired resolution. In the NWRT PAR, the size of the azimuthal sector is limited by electronic beam steering to  $\pm 45^\circ$  relative to boresite.

The required vertical resolution and extent of coverage determines the sampling in elevation. Usually finer vertical resolution is desired closer to the ground, but due to the inherent coordinate system or the radar sampling grid, vertical resolution varies as a function of range. Storm tops and their range may be used to determine the highest elevation angle of beam positions needed to sample an entire storm. As such, nearby storms would require larger elevation spans and vice versa. In the NWRT PAR, elevation angles can range from 0.5 to 60°.

In addition to being dependent on the number of beam positions, the scan update time is also directly proportional to the dwell times defined by the scanning strategy. The dwell time is the time spent at a given beam position; it depends on the waveform, PRT(s), and desired number of samples (pulses). In the NWRT PAR, available waveforms are uniform PRT, batch PRT, staggered PRT, and beam multiplexing (BMX). The PRT controls the maximum unambiguous range and velocity, but different waveforms, such as staggered PRT, can be used to mitigate ambiguities (e.g., Torres et al. 2004). In the NWRT PAR, the PRT can range from 0.8 ms to 3.2 ms. Dwell times can be reduced by reducing the PRT(s) or the number of samples. However, in general, shorter dwell times result in reduced data quality. In addition, reducing the PRT may increase the likelihood of overlaid echoes, and reducing the number of samples can affect the performance of some signal processing techniques, such as ground clutter filtering, which require a minimum number of samples for adequate suppression.

In summary, the scan update time can be reduced by reducing either the number of beam positions or dwell times. That is, achieving faster data updates leads to a tradeoff between spatial resolution and data quality. Nevertheless, there are techniques that can be used to reduce dwell times without a sacrifice in data quality. For example, range oversampling techniques (Torres and Zrnić 2003) use faster sampling rates at the radar receiver so that more samples are acquired in range without increasing the dwell times; range samples collected in this way can be decorrelated and used to reduce the errors of estimates via averaging. Conversely, dwell times can be increased without increasing the update time. Beam multiplexing (Yu et al. 2007) exploits beam agility to "multitask" by interlacing the sampling of multiple beam positions, which leads to longer dwell times without increasing the overall scan update time.

#### a. Design tradeoffs

As introduced above, the design of effective scanning strategies for a particular situation must balance a number of tradeoffs. Above all, scanning strategies must be compatible with operations in terms of both processing and consumption of radar data. For example, a scanning strategy that employs BMX would not be compatible with traditional ground clutter filters due to the nonuniform sampling of time-series data. Also, less traditional spatial sampling in scanning strategies, such as range height indicator (RHI) scans, may not be compatible with standard displays of radar data. Nevertheless, after operational compatibility is attained, any scanning strategy design requires data quality, spatial resolution, and update time tradeoffs. Data quality is often dictated by strict requirements that must be maintained to produce timely and useful data for forecasters and automatic algorithms. The spatial resolution of radar data determines the ability to detect small-scale phenomena. On the other hand, the scan update time relates to the potential to detect fast-evolving phenomena. In conclusion, update time can be traded for data quality and/or spatial resolution and the best compromise depends on the particular consumer (user or algorithm) of radar data.

#### b. Design criteria

The concept of designing custom scanning strategies is not unique to PAR-based systems. For instance, the WSR-88D network uses precipitation and clear-air scanning strategies with different tradeoffs (NOAA 2006); three examples follow. Precipitation volume coverage pattern (VCP) 21 comprises 9 elevation tilts (0.5 to 19.5°) and employs long dwell times resulting in a 6-min scan update. This scanning strategy trades improved data quality for slower update times and coarser vertical sampling. Precipitation VCP 12 comprises 14 tilts (0.5 to 19.5°) and employs short dwell times resulting in a ~4-min scan update. This strategy trades faster updates and denser vertical sampling at the lower tilts for reduced data quality. Clear-air VCP 31 comprises 5 tilts (0.5 to 4.5°) and employs long dwell times with a 10-min scan update. This strategy trades improved detection and better data quality for slower update times and limited vertical sampling.

Similarly, for NWRT PAR we have adopted phenomenon-specific scanning strategies. These achieve the best tradeoffs for a particular situation. Improved spatial resolution is achieved with scanning strategies employing

higher-resolution vertical sampling and/or azimuthal sampling. Unique to the PAR is that the inherent beam broadening can be exploited to reduce the number of beam positions and obtain faster updates (e.g., to completely cover a 90-deg sector, only 55 non-overlapping radials are needed). For improved temporal resolution there are different options. BMX can be exploited to produce good data quality with faster updates. Yu et al. (2007) report it is possible to reduce the scan time by a factor of 2 to 4 without an increase in the errors of estimates at high signal-to-noise ratios. The tradeoff is in terms of data quality since effective ground clutter filters that are compatible with BMX have yet to be developed.

More frequent updates for the lowest tilt are achievable by adding a low-elevation scan half way through the scanning strategy. This results in good data quality, but faster updates are only realized at the lowest tilt and this leads to slightly slower updates elsewhere. Through elevation-prioritized scanning different updates at different levels can be achieved. In general, the fastest updates occur at the lowest tilts for the best temporal resolution closer to the ground. Intermediate tilts are updated less frequently, enough to detect new storm developments with short latency. Finally, the upper tilts get the slowest updates. Another way to improve the temporal resolution of the NWRT PAR without loss in data quality is to scan less than the full 90°. However, new developments outside the reduced sector are likely to be missed. An optimum compromise to produce good-quality data with faster updates is to employ adaptive scanning techniques that automatically focus data collection on smaller areas of interest at the same time that periodic surveillance is performed to capture new storm developments. This automatic algorithm is described in the next section.

#### 4. ADAPTS: Adaptive Data Signal Processing Algorithm for PAR Timely Scans

ADAPTS is a proof-of-concept implementation of spatially targeted adaptive scanning for the electronically steered NWRT PAR. Preliminary evaluations of ADAPTS have shown that the performance improvement with electronic adaptive scanning can be significant compared to conventional scanning strategies, especially when observing isolated storms as illustrated in section 5. ADAPTS works by turning “on” or “off” individual beam positions within a scanning strategy based on three criteria. If one or more criteria are met, the beam position is declared active. Otherwise, the beam position is declared inactive. Active beam position settings are applied and become valid on the next

execution of a given scanning strategy. Additionally, ADAPTS periodically completes a complete volumetric surveillance scan, which is used to redetermine where weather echoes are located. A user-defined parameter controls the time between full surveillance scans (by default this is set at 5 min). Following a surveillance scan, data collection continues only on the active beam positions.

A beam position becomes active if one or more of the following criteria are met: (1) reflectivities along the beam meet continuity, coverage, and significance conditions; (2) the elevation angle is below a predefined level; or (3) a “neighboring” beam position is active based on the first or second criteria. The first criterion uses continuity, coverage, and significance conditions to make a quantitative determination of the amount of significant weather returns at each beam position. In this context, a beam position is active if it contains: (a) a certain number of consecutive range gates (by default 4) with reflectivities exceeding a threshold (by default 10 dBZ), and (b) a total areal coverage (by default 1 km<sup>2</sup>) with reflectivities exceeding the same threshold. The second criterion provides data collection at all beam positions for the lowest elevation angles to monitor low-altitude developments. A user-defined elevation threshold (2.5° by default) controls the lowest elevation angle where ADAPTS may begin to deactivate beam positions. The third criterion uses “neighboring” beam positions to expand the data collection footprint to allow for continuous adaptation in response to storm advection, growth, or decay. Nevertheless, new developments at midlevels may not be immediately sensed, and therefore additions to the list of active beam positions may be delayed until the next full surveillance volume scan. Neighboring beam positions are defined as those immediately above and below in elevation and two on either side in azimuth of an active beam position (i.e., there are a total of 6 neighbors for each beam position, unless the scanning domain boundaries are approached). If no beam positions are defined active above the user-defined elevation threshold (criterion 2), ADAPTS will activate all beam positions at the tilt directly above the elevation threshold.

At the time of this writing, ADAPTS only works with scanning strategies that have a specific structure. ADAPTS assumes that there is only one PPI scanning strategy that repeats continuously. The algorithm also expects that all tilts are ordered in ascending elevation order, and use the same azimuth beam positions with a minimum azimuthal spacing of 0.5° (i.e., the maximum number of beam positions in an elevation is 180). These limitations will be

removed with the next upgrade cycle scheduled for the Spring of 2010.

Users at the RCI can monitor the performance of the ADAPTS algorithm by looking at a graphical display of active beam positions (Fig. 1). Beam positions are color-coded as follows: white beam positions are inactive, green and yellow beam positions are active. Green beam positions meet the first and second detection criterion, whereas yellow beam positions correspond to the “neighbor” footprint extension (third criterion). The display updates every second and highlights in red the “current” beam position.

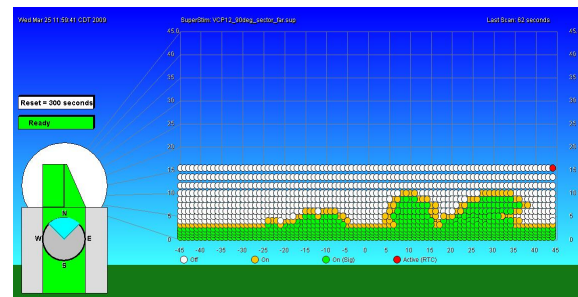


Fig. 1. Depiction of ADAPTS’ real-time performance at the NWRT PAR user interface. Beam positions on an azimuth-by-elevation plane are color-coded as follows: white beam positions are inactive, green beam positions are active based on elevation and coverage criteria, and orange beam positions are active based on the neighborhood criterion.

## 5. ILLUSTRATIONS OF SAMPLING TRADEOFFS WITH THE NWRT PAR

One of the key advantages of NWRT PAR is the capability to produce the higher-temporal resolution data desired by NWS forecasters (e.g., Steadham 2008), broadcast meteorologists in the Southern Plains (LaDue et al. accepted), and several government agencies (OFCM 2006). Multipanel designs typical of PAR systems reduce sampling time by each panel scanning only part of a 360° sector (Brookner 1988). This type of design is demonstrated by the 90° sector scanned by the NWRT PAR. As discussed in section 3, though, depending on the situation, update time can be traded for spatial resolution and/or data quality. This section uses case examples to illustrate some of the sampling tradeoffs employed by the NWRT PAR for scanning storms.

*a. Trading update time for higher-resolution vertical sampling*

When WSR-88D VCPs are employed by the NWRT PAR, temporal resolution is improved by a factor of four due to the smaller sector size: 90° vs 360°. Sampling storms with VCPs 11 and 12, for example, results in updates of 1.25 and 1.0 min, respectively. Given this significant improvement in temporal sampling, a relevant research question is: in what situations might it be worthwhile to reduce the temporal sampling rate to improve observations of vertical storm structures?

To study this question, a scanning strategy with 25 tilts, spaced to provide a vertical overlap of up to one-half beamwidth, was developed and implemented in spring 2009. Rather than designing a “one-size-fits-all” scanning strategy, two versions were developed to better sample the vertical structure of storms located near and far from the radar (Fig. 2). The near-version extended to 28.5° to provide more detailed sampling through higher heights than typical scanning strategies. In contrast, the far-version (radar range  $\geq 80$  km) extended to only 16.1° to avoid scanning above storm top height (assumed  $\leq 18$  km AGL), while providing even denser vertical sampling than the near scan (Fig. 2). In both versions the number of samples either matched or exceeded those of VCP 12 (NOAA 2006), and the PRTs were chosen to match the maximum expected range of storms. Slight adjustments to the PRTs and number of samples achieved the same update time for both versions. Data were collected using a batch PRT waveform and 1° azimuthal oversampling. This combination of scanning strategy characteristics produced an update time of  $\sim 2$  min.

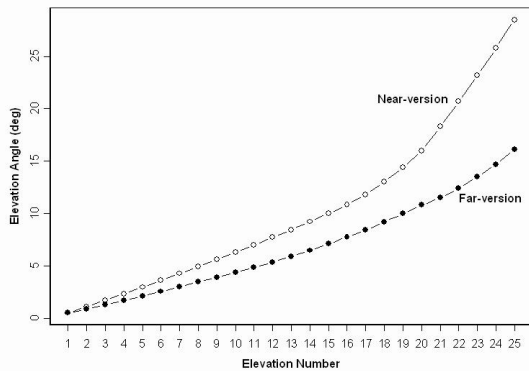


Fig. 2. The 25 elevation angles that define the near- (open circles) and far-versions (filled circles) of the dense vertical scanning strategy.

One radar-derived application that could benefit from dense vertical sampling is storm-top height estimates. In this study, storm-top height is

defined as the highest height at which 18 dBZ or higher reflectivity factor is sampled. Because uncertainty in storm-top height estimates is related primarily to the spacing between consecutive tilts, closer spacing reduces uncertainty. The impact of dense vertical sampling on storm top estimates is illustrated in Fig. 3. In this case, a group of longitudinally oriented storms, located about 100 km from the NWRT PAR, were sampled at  $\sim 0352$  UTC 13 May 2009 using the far-version of the dense vertical scanning strategy (Fig. 2). Typically, the upper-levels of storms (in this case 11–15 km MSL) located 100 km from the radar would be sampled by two elevation angles (2°-increment) rather than by four (Fig. 3). If these two elevation angles were 6.48° and 8.46°, storm-top height estimates would be 14.9 km MSL for storm A and 11.8 km MSL for storms B–E. The dense vertical sampling better captures variations in storm-top height among storms A through E (Fig. 3) and reduces the uncertainty of estimates. The storm-top heights resulting from denser vertical sampling are A: 14.9 km, B: 13 km, C: 14 km, D: 12.6 km, and E: 11.8 km MSL. As mentioned earlier, the trade-off for dense vertical sampling is longer sampling time (2 vs 1 min).

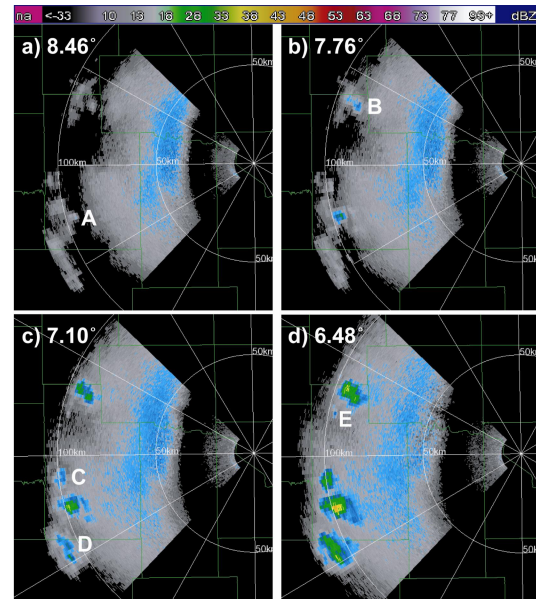


Fig. 3. Storm-top heights (18 dBZ echo) depicted by dense vertical sampling at  $\sim 0352$  UTC 13 May 2009. Elevation angles are (a) 8.46°, (b) 7.76°, (c) 7.10°, and (d) 6.48°. Letters denote the tilt at which storm top height was computed. Range rings are shown in 50-km increments.



*b. Trading update time for higher-resolution azimuthal sampling*

The depiction of velocity signatures with significant gradients in the azimuthal direction depends strongly on azimuthal sampling. Similar to super-resolution sampling (Brown et al. 2002), 50% overlapped azimuthal sampling ( $0.75\text{--}1.05^\circ$ ) was employed to improve the resolution of azimuthal signatures sampled by the NWRT PAR. Because the beamwidth varies across the sector, the oversampling is adjusted accordingly. In this case, the increased number of azimuthal beam positions (55 without oversampling; 109 with 50% oversampling) at all elevations (14) increases the sampling time of the VCP. These sampling characteristics increased the volumetric sampling time from about 1 min to approximately 1.4-min.

A key velocity signature that can benefit from high-resolution azimuthal sampling is the mesocyclone signature. At 0131:24 UTC 1 May 2009, the NWRT PAR sampled the center of a mesocyclone signature located  $\sim 170$  km west-northwest of the NWRT PAR (Fig. 4). At this location the azimuthal sampling spacing without oversampling was  $\sim 4.63$  km, whereas with 50% oversampling the azimuthal sampling spacing was  $\sim 2.31$  km. To simulate velocity and reflectivity fields without azimuthal oversampling, every other radial was removed from the oversampled data and then plotted for comparison. The comparison of the structure of the mesocyclone signature in the velocity field, and the structure of the inflow notch and hook echo in the reflectivity field shows that these structures are more poorly resolved when azimuthal oversampling is not employed (Fig. 4).

The improved vertical and azimuthal spatial resolution illustrated in Figs. 3 and 4 came at the expense of slower update times. The remaining subsections describe three scanning methods that can achieve the high-temporal resolution sampling needed to observe rapid evolution in severe storms.

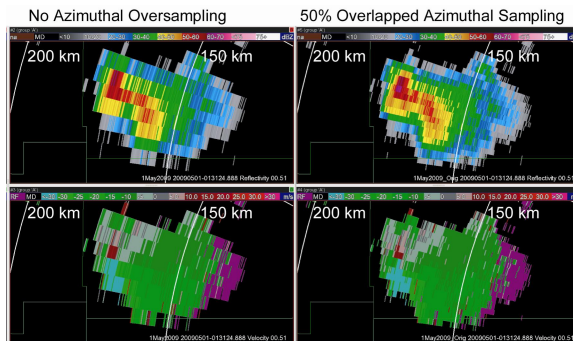


Fig. 4. Comparison of velocity and reflectivity fields at  $0.5^\circ$  elevation with no azimuthal oversampling (left panel) and 50% overlapped azimuthal sampling (right panel).

*c. Achieving high-temporal resolution data with beam multiplexing (BMX) and sector scanning*

On 19 August 2007 low-top supercells developed in a tropical environment, rarely experienced in Oklahoma, a few hours prior to the reintensification of tropical cyclone Erin (Arndt et al. 2009). Due to the potential for tornado development, both high-temporal resolution sampling ( $< 1$  min) and accurate estimates of radial velocity were desired. This goal was accomplished by implementing a BMX scanning strategy with the same 14 tilts as the NEXRAD VCP 12 (NOAA 2006). Accurate velocity and reflectivity estimates were obtained by sampling the storm with 64 pulses at all elevations. Velocity aliasing and update time were minimized by employing a uniform and lowest available PRT (0.8 ms). In this case, the uniform PRT was appropriate due to the lack of storm development beyond 120 km. The azimuthal sampling spacing of velocity estimates was improved by fixed  $0.5^\circ$  oversampling. Without BMX, these scanning strategy characteristics would typically produce 132-s volumetric updates over a  $90^\circ$  sector. The implementation of BMX increased the temporal resolution by approximately a factor of 2, resulting in 63-s updates. In the example shown, the update time was reduced further, from 63 s to 43 s, by decreasing the sector size to  $60^\circ$  (Fig. 5). The smaller sector size focused data collection on a low-top supercell located  $\sim 60$  km from the NWRT PAR (Fig. 5a). At this radar range, the height of the  $0.5^\circ$  tilt was 0.8 km MSL and the spatial distance between azimuthal observations was 0.52 km.

The 43-s volumetric sampling captured the development of a cyclonic velocity couplet at the  $0.5^\circ$  elevation during 0141:27–0143:36 UTC 19 August 2007 (Fig. 5b). A damage survey later revealed that about 2 min after the velocity couplet first appeared on the NWRT PAR (Fig. 5c), a short-lived ( $\sim 2$  min) tornado occurred that produced EF1 damage along a swath 2.0-km long and 0.036-km wide (<http://ewp.nssl.noaa.gov/projects/shave/tornsurvey.php#map>). During the tornado's short lifetime, the maximum measured gate-to-gate azimuthal velocity difference was  $48\text{ m s}^{-1}$ . The rapid development and short-lived nature of this tornado illustrates the need for high-temporal resolution data to sample this type of event. As mentioned previously, a drawback of this scanning strategy is that ground clutter filtering is

currently unavailable for BMX. However, this was not an issue in this particular case because the storm of interest was located beyond the typical clutter field for the NWRT PAR.

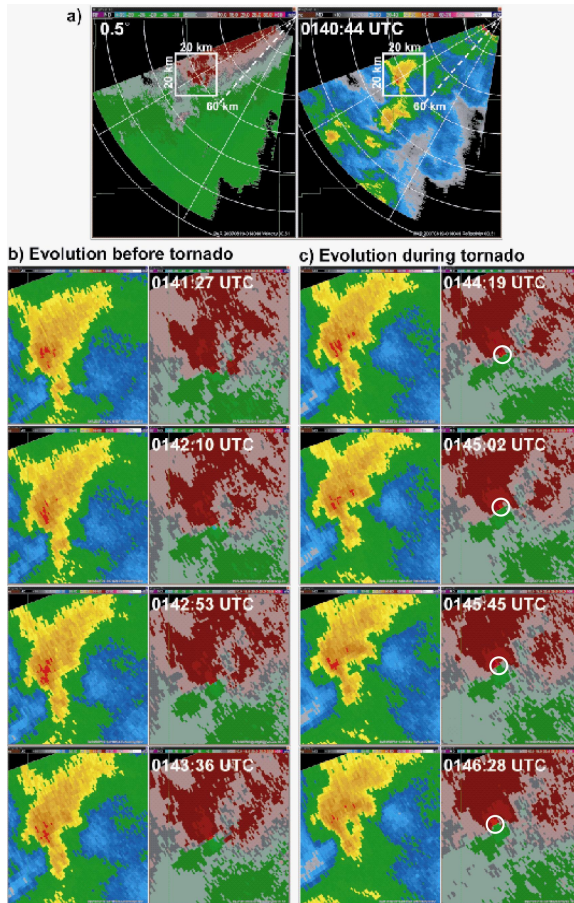


Fig. 5. (a) A 60° sector scan of 0.5°-elevation reflectivity and velocity fields at 0140:44 UTC 19 August 2007. Range rings are in 20-km increments. The white box denotes the location and scale of the storm whose evolution at the 0.5° tilt is shown (b) prior to and (c) during an EF1-rated tornado, whose location and duration was determined by the associated damage survey. The white circle encloses the tornadic vortex signature.

*d. Elevation-prioritized scanning for rapid-updates at low elevation angles*

Elevation-prioritized scanning is designed to provide the fastest update rate at low-elevation angles and the slowest update rate at high-elevation angles. In this case, 14 tilts are elevation-prioritized to accomplish the following within about 4 min (Fig. 6):

- 6 updates at the lowest 2 elevations,

- 3 updates at the next 5 elevations, and
- 2 updates at the 6 highest elevations.

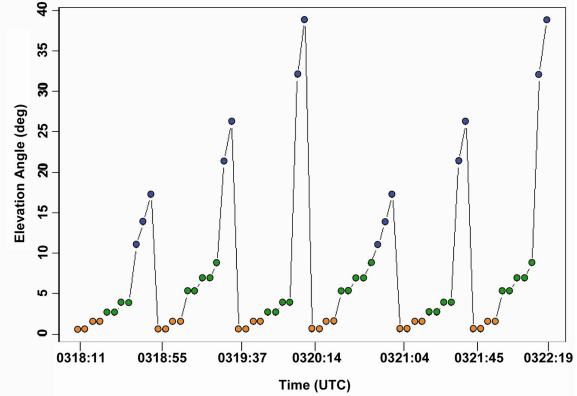


Fig. 6. Temporal order of elevation angles in near-version of elevation-prioritized scanning strategy. The median temporal resolution is indicated by the colored dots: orange: 43.5 s (0.73 min), green: 87s (1.45 min), blue: 132.5 s (2.2 min).

Due to the interlaced nature of this scanning strategy, the temporal sampling rate at a fixed elevation angle varies. The time intervals between 0.5°-elevation scans, for example, range from 41 to 51 s, with a median time interval of 43.5 s. The median update times for the elevation-prioritized scanning strategy are as follows: the lowest two elevation angles 43.5 s (0.73 min), the middle elevation angles 87 s (1.45 min), and upper-elevation angles 132.5 s (2.2 min).

Like the dense vertical scanning strategy, the elevation-prioritized scanning strategy has two versions: near and far. Only the near-version is described in detail (Fig. 6) because the storm in the case example was located within 50 km of the NWRT PAR. Both versions, however, operate similarly with the main difference being the specific elevation angles and PRTs employed.

The update times result from the number and temporal ordering of the elevation angles, the PRTs, azimuthal sampling, and number of pulses. To improve azimuthal sampling, the elevation-prioritized scanning strategy implements 50% overlapped azimuthal sampling at all elevation angles. To further improve detection of tornadic vortex signatures and other hazardous weather signatures, velocity errors at the lowest two tilts are minimized by collecting a relatively high number of pulses (64).

The accuracy of reflectivity data is also enhanced by collecting more than the traditional number of pulses (16) for all surveillance scans. The higher number of pulses provides less noisy depictions of hook echoes, bounded weak echo regions, and other reflectivity signatures associated with potentially severe convective storms.

On the evening of 13 May 2009 (CDT) a cyclic supercell moved across Oklahoma City, Oklahoma. Because tornado occurrence was a concern, high-temporal resolution sampling, especially at the lower elevations, was desired. As noted earlier, due to the storms' proximity to the NWRT PAR, the supercell was sampled with the near version of the elevation-prioritized scanning strategy (Fig. 6), which provided 43.5 s median updates at the two lowest elevations: 0.5° and 1.5°. These data were collected while the supercell's hook echo and several mesocyclone circulations were located within 10 to 20 km of the NWRT PAR during 0318:11–0348:26 UTC 14 May 2009.

At 0339:25 UTC, a prominent cyclonic circulation at the 0.5° elevation was sampled by 0.22-km azimuthal spacing at a height of 0.5 km MSL (Fig. 7). To track the intensity of the initial and subsequent circulations, the maximum azimuthal velocity difference within 1 km of the circulations' center was computed. Though the velocity difference associated with this first circulation was  $23.5 \text{ m s}^{-1}$  at 0339:25 UTC, it rapidly dissipated within the following 2 min. Within this same time interval, a new circulation developed ~1 km to the north of the former one (0341:00 UTC, Fig. 7). The initial velocity difference of this second cyclonic circulation was  $26 \text{ m s}^{-1}$  (0341:00 UTC); this intensity was maintained or exceeded during the next 5 min.

A comparison of the locations of this velocity signature with a damage survey (completed by the first author and Les Lemon, who is affiliated with the Warning Decision Training Branch) concluded that a short-lived tornado producing EF0 damage occurred during the 0342:24 and 0343:50 UTC volume scans (Fig. 7). During its short duration, the maximum measured velocity difference was  $31.5 \text{ m s}^{-1}$  (0.5 km MSL) at 0343:50 UTC. Within the tornado's lifetime, it crossed the marina on the western shore of Lake Stanley Draper and proceeded southward across a picnic area, parking lot, and walking path just east of a small pond, producing an approximate 0.80-km long damage path. Once again, the rapid development and short-lived nature of this tornadic event illustrates the need for high-temporal resolution radar data to detect the occurrence of similar types of events.

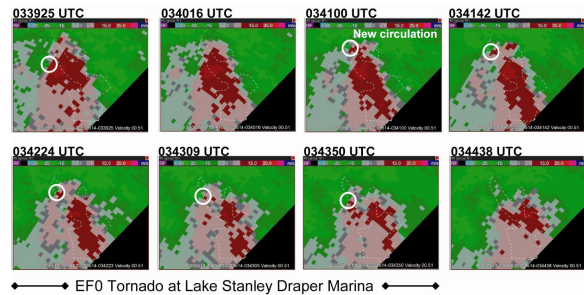


Fig. 7. A time series of NWRT PAR 0.5°-elevation radial velocity data prior to and during the EF0 tornado over Lake Stanley Draper. The white circle highlights the two significant cyclonic circulations discussed in the text.

#### e. Adaptive scanning

During 0040:59–0044:03 UTC 1 May 2009, data were collected on an isolated storm located in Custer County, Oklahoma (Fig. 8a). The storm developed into a nontornadic supercell that, according to a preliminary Storm Data report, produced up to baseball-size hail stones (2.75 in) at approximately 0200 UTC near Stafford, Oklahoma in south-central Custer County (<http://www.spc.noaa.gov>). Because the storm was isolated, it was a good candidate for demonstrating and evaluating the potential utility of ADAPTS. As described in section 4, a primary goal of ADAPTS is to reduce scan time by sampling only regions containing weather echoes, while capturing the growth, decay, and horizontal advection of existing storms. When ADAPTS is running, full volume scans are collected at ~5-min intervals, with adaptive scanning occurring between them. Due to the storm's distance from the PAR, 150 to 200 km, and a desire for rapid updates at all tilts, the storm was sampled with a far-version of a conventional 14-tilt scanning strategy that extended to 15.5°. Like several of the other scanning strategies, this one employed 50% overlapped azimuthal sampling at all elevations; the PRTs ranged from 0.8 to 3.104 ms. These sampling characteristics resulted in approximately 1.4-min updates.

Fig. 8b shows the improvement in temporal resolution attained from ADAPTS. The occasional gaps in the time series indicate loss of data collection owing to rebooting the radar control interface. The highest improvement in temporal resolution, 0.9 min, occurs early in the



storm's life time: 0040:59 – 0052:44 UTC. Over the next hour, volume updates of 1 min or less are maintained between volume scans (Fig. 8b). Thereafter, Fig. 8b shows a nearly linear increase in sampling time between 5-min intervals, which directly corresponds to an increase in the number of active beam positions. The contributing factors to the increase in active beam positions were an increase in the number of storms sampled and horizontal (Fig. 8a) and vertical (not shown) storm growth as the storms advanced toward the NWRT PAR.

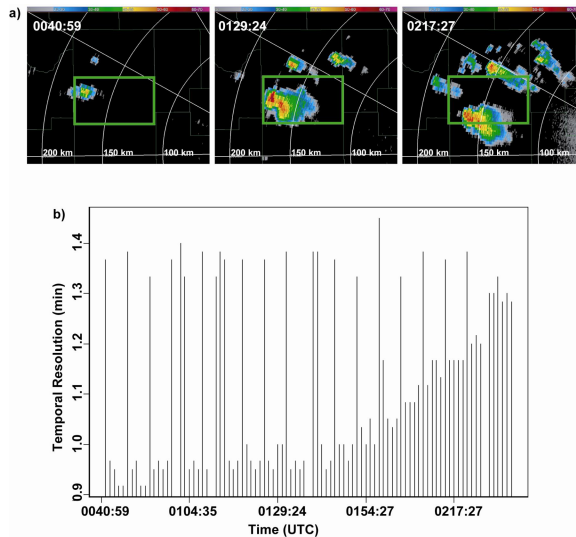


Fig. 8. (a) Three 0.5°-elevation reflectivity images illustrating the evolution of areal storm coverage on 1 May 2009. The green box outlines Custer County in west-central Oklahoma. (b) Time series showing temporal resolution of 102 volume scans collected within 0040:59 – 0244:03 UTC 1 May 2009. Blank areas within the time series indicate a break in data collection.

## 5. Conclusions

The focus of this work was the capability to observe weather phenomena with high-temporal resolution. The tradeoffs that exist when designing scanning strategies were discussed. We presented examples of scanning strategies that trade update time for coverage and/or data quality and illustrated each of these with case data. The examples show that having phenomenon-based, adaptive scanning strategies is essential to fully capitalize on the benefits of PAR technology in a multifunction environment in which radar resources are shared by multiple tasks.

Although a comprehensive study of the improvements resulting from high-temporal sampling of weather phenomena was beyond the

scope of this study, it was demonstrated that PAR technology can be exploited to achieve results that are unfeasible with current operational technology. Nonetheless, more research is needed to translate these improvements into concrete, measurable, and meaningful service improvements for the National Weather Service. As such, the NWRT PAR will continue to explore and demonstrate new capabilities to address 21st century weather forecast and warning needs.

**Acknowledgements:** The authors are grateful for the data collection efforts of NSSL staff and thank NSSL radar and software engineers for advances in data quality and radar functionality that made this research possible. We also appreciate the technical expertise of Kurt Hondl and Valliappa Lakshmanan in the display of phased array radar data. This manuscript benefited from reviews from Rodger Brown, Dick Doviak, and Dusan Zrnić and was prepared with funding provided by NOAA/Office of Oceanic and Atmospheric Research under NOAA-University of Oklahoma Cooperative Agreement #NA17RJ1227, U.S. Department of Commerce. The statements, findings, conclusions, and recommendations are those of the author(s) and do not necessarily reflect the views of NOAA or the U.S. Department of Commerce.

## References

- Arndt, D. S., J. B. Basara, R. A. McPherson, B. G. Illston, G. D. McManus, and D. B. Demko, 2009: Observations of the overland reintensification of Tropical Storm Erin (2007). *Bull. Amer. Meteor. Soc.*, **90**, 1079–1093.
- Brown, R. A., V. T. Wood, and D. Sirmans, 2002: Improved tornado detection using simulated and actual WSR-88D data with enhanced resolution. *J. Atmos. Oceanic Technol.*, **19**, 1759–1771.
- Doviak, R., and D. Zrnić, 2006: *Doppler Radar and Weather Observations*. 2<sup>nd</sup> ed. Academic Press, 562 pp.
- Heinselman, P. L., D. L. Priegnitz, K. L. Manross, T. M. Smith, and R. W. Adams, 2008: Rapid sampling of severe storms by the National Weather Radar Testbed Phased Array Radar. *Wea. Forecasting*, **23**, 808–824.
- Junyent, F., V. Chandrasekar, D. McLaughlin, E. Insanic, and N. Bharadwaj, 2010: The CASA Integrated Project 1 networked radar

- system. *J. Atmos. Oceanic Technol.*, in press.
- LaDue, D., P. Heinselman, and J. Newman, 2009: Strengths and limitations of current radar systems for two stakeholder groups in the Southern Plains. *Wea. Forecasting*, accepted.
- National Academies, 2008: Evaluation of the multifunction phased array radar planning process. Report prepared by the National Research Council, National Academy of Science, National Academy Press, 79 pp.
- NOAA, 2006: Doppler radar meteorological observations. Part C: WSR-88D products and algorithms, Chapter 5. Federal Meteorological Handbook, FCH-H11C-2006, Office of the Federal Coordinator for Meteorological Services and Supporting Research, Rockville, MD, 23 pp.
- OFCM 2006: Federal research and development needs and priorities for phased array radar, FMC-R25-2006, Interdepartmental Committee for Meteorological Services and Supporting Research, Committee for Cooperative Research Joint Action Group for Phased Array Radar Project, 62 pp.
- Steadham, R., 2008: *2008 National Weather Service Field Study. Part 1: Volume Coverage Pattern Usage*. Radar Operations Center, Norman, OK, 28 pp. [Available from WSR-88D Radar Operations Center, 1200 Westheimer Dr., Norman, OK 73069]
- Torres, S., and D. Zrnčić, 2003: Whitening in range to improve weather radar spectral moment estimates. Part I: Formulation and simulation. *J. Atmos. Oceanic Technol.*, **20**, 1433-1448.
- Torres, S., and C. Curtis, 2007: Initial implementation of super-resolution data on the NEXRAD network. Preprints, *23rd International Conference on Interactive Information and Processing Systems (IIPS) for Meteorology, Oceanography, and Hydrology*, San Antonio, TX, Amer. Meteor. Soc., Paper 5B.10.
- Torres, S., Y. Dubel, and D. Zrnčić, 2004: Design, implementation, and demonstration of a staggered PRT algorithm for the WSR-88D. *J. Atmos. Oceanic Technol.*, **21**, 1389–1399.
- Torres, S., R. Adams, C. Curtis, E. Forren, I. Ivić, D. Priegnitz, J. Thompson, and D. Warde, 2010: Update on signal processing upgrades for the National Weather Radar Testbed Phased-Array Radar. *25<sup>th</sup> International Conference on Interactive Information and Processing Systems (IIPS) for Meteorology, Oceanography, and Hydrology*, Atlanta, GA, Amer. Meteor. Soc., 14B.2.
- Weber, M. E., J. Y. N. Cho, J. S. Herd, J. M. Flavin, W. E. Benner, and G. S. Torok, 2007: The next-generation multimission U.S. surveillance radar network. *Bull. Amer. Meteor. Soc.*, **88**, 1739–1751.
- Yu T.-Y., M. B. Orescanin, C. D. Curtis, D. S. Zrnčić, and D. E. Forsyth, 2007: Beam multiplexing using the phased-array weather radar. *J. Atmos. Oceanic Technol.*, **24**, 616–626.
- Zrnčić, D. S., J. F. Kimpel, D. E. Forsyth, A. Shapiro, G. Crain, R. Ferek, J. Heimmer, W. Benner, T.J. McNellis, R.J. Vogt, 2007: Agile beam phased array radar for weather observations. *Bull. Amer. Meteor. Soc.*, **88**, 1753–1766.